

**Photocatalytic degradation of methylene blue by WO<sub>3</sub> prepared via a very simple precipitation method under visible light irradiation**

**Rahmatollah Rahimi, Mahboubeh Rabbani\*, Maryam Mosaffa**

*Department of Chemistry, Iran University of Science and Technology, Narmak, Tehran 16846-13114, Iran*

*(E-mail: [m\\_rabani@iust.ac.ir](mailto:m_rabani@iust.ac.ir))*

**Abstract**

Tungsten oxide (WO<sub>3</sub>) nanoparticles have been synthesized by a simple precipitation method and utilized as photocatalyst for degradation of methylene blue (MB) dye under LED-visible light irradiation. This photocatalyst was characterized by X-ray diffraction (XRD), scanning electron microscopy (SEM), Fourier transform infrared (FTIR) spectroscopy and UV-visible spectroscopy to determine phase, morphology, vibration mode, and optical property.

**Introduction**

Semiconductor photocatalysis has been extensively studied as a viable water treatment method [1]. Although the TiO<sub>2</sub>/UV process has been most frequently studied for this purpose, visible light active photocatalysts are being actively sought for better utilization of solar light [2,3]. Among many visible active photocatalysts, tungsten oxide (WO<sub>3</sub>) is an ideal candidate because of its small band gap (2.4-2.8 eV), high oxidation power of valence band (VB) holes (+3.1-3.2 VNHE), nontoxicity, and stability (4-6).

The  $\gamma$ -monoclinic structure of WO<sub>3</sub> results from a slight distortion of the cubic structure, with the corner-sharing WO<sub>6</sub> octahedra tilted. One can look at it as a 2×2×2 superstructure based on an idealized cubic unit cell, or, alternatively as consisting of pseudo-one-dimensional weakly

interacting -W-O-W- chains. The computed direct bandgap is 3.10 eV; experimentally, values in the range 2.6-3.0 eV have been reported [7] The upper part of the VB is mainly derived from the O2p states. The bottom of the CB is mainly composed of W5d states partly mixed in with O2p orbitals. Owing to a distorted-octahedral coordination, the W5d states split into  $t_{2g}$  and  $e_g$ -like components (Fig. 1). As the W-O bond lengths are asymmetric along both y and z directions while are nearly symmetric along the x direction [8] the lower energy  $t_{2g}$  states further split into  $d_{yz}$  and  $d_{xz}/d_{xy}$  components. Thus, it can be expected that a distortion of the  $WO_6$  octahedron and in particular a change in W-O bond lengths can affect both the splitting of  $t_{2g}$  states as well as the position of the CB bottom [9].

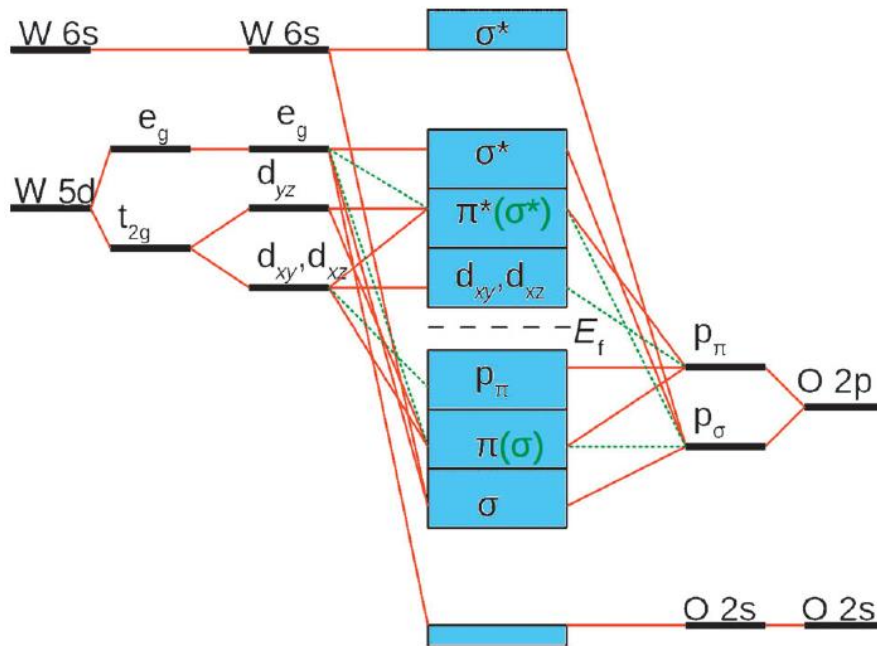


Fig. 1. The schematic representation of  $WO_3$  electronic energy levels starting from atomic orbitals [9].

In this work, we assembled WO<sub>3</sub> nanopowders prepared through a co-precipitation method. The methylene blue was used as model pollutants to investigate the photocatalytic characteristics of WO<sub>3</sub> in aqueous system.

## **Materials and methods**

All the chemicals purchased from Merck were of analytical grade and used without further purification. Firstly, sodium tungstate dihydrate (Na<sub>2</sub>WO<sub>4</sub>·2H<sub>2</sub>O) was dissolved in the equal volume ratio of distilled water and nitric acid taken together to prepare 0.1 M solution. Then, the solution was stirred for 15 h at room temperature, and the whole solution was kept for 20 h for aging. Finally, the obtained yellow precipitate was separated and washed with distilled water several times to remove impure ions completely from the precipitate. The resulting precipitate was dried at 60 °C and then calcined at 500 °C for 2 h in air.

## **Characterization of WO<sub>3</sub> nanopowder**

Scanning electron microscopy (SEM) analysis of as-prepared sample was carried out using Tescan MIRA3 scanning electron microscope to examine the surface morphology. X-ray diffraction patterns for bioadsorbent was obtained using Philips X'pert Pro diffractometer with 2 $\theta$  range of 10 to 60 and step size of 0.05. The amount of residual dye in the solution was traced by UV-vis spectra (ShimadzuUV-1700), and the dye concentration was calculated by the absorbance at the maximum absorption.

## **Photocatalytic activity measurement**

The photocatalytic activities of samples were evaluated by measuring the photodegradation of methylene blue (MB). In a typical measurement, 20 mg photocatalysts were suspended in 20 mL of 25 ppm aqueous solution of MB. The suspension was stirred and illuminated with a 5 W LED lam. The concentration change of MB was monitored by measuring the UV-Vis absorption of the suspensions at regular intervals. The suspension was centrifuged for 5 min to remove the photocatalysts before measurement. The peak absorbance of MB at 664 nm was used to determine its concentration. The dye removal and adsorbed amount were determined according to the following:

$$\text{Dye removal (\%)} = \frac{C_0 - C}{C_0} \times 100$$

where  $C_0$  and  $C$  ( $\text{mg.L}^{-1}$ ) are the initial and final concentration of MB, respectively.

## **Results and discussion**

### **Catalyst Characterization**

Comparing the XRD patterns from the JCPD reference files, the diffraction peaks are in agreement with a Monoclinic structure (JCPD=24-0747, space group: P21/n). The diffraction peaks corresponded to (0 2 0), (2 0 0), (1 2 0), (-1 1 2), (1 1 2), (0 2 2), (-2 0 2), (2 2 0), (4 0 0) and (-1 1 4) planes of crystalline  $\text{WO}_3$  by monoclinic structure (Fig. 2).

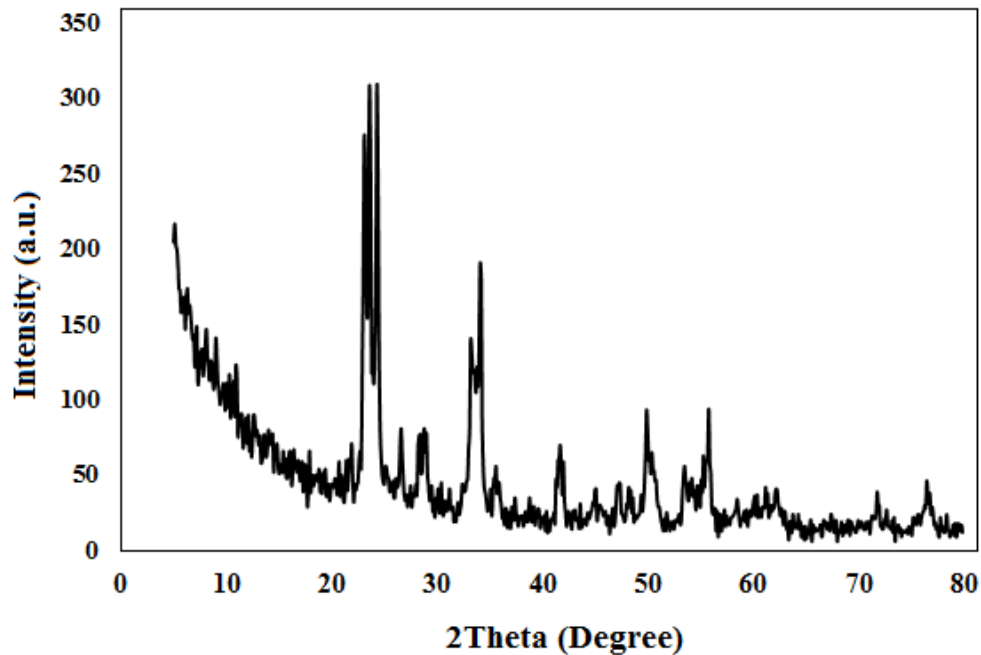


**Fig. 2.** The XRD plot of the synthesized  $\text{WO}_3$ .

In the spectrum of the  $\text{WO}_3$  (Fig. 3) a weak band located at  $3416\text{ cm}^{-1}$  is assigned to stretching modes of OH groups. A band at  $672\text{ cm}^{-1}$  and broad band at  $837\text{ cm}^{-1}$  can be assigned to the  $\nu(\text{O}-\text{W}-\text{O})$  and  $\nu(\text{W}=\text{O})$  vibrations, respectively.

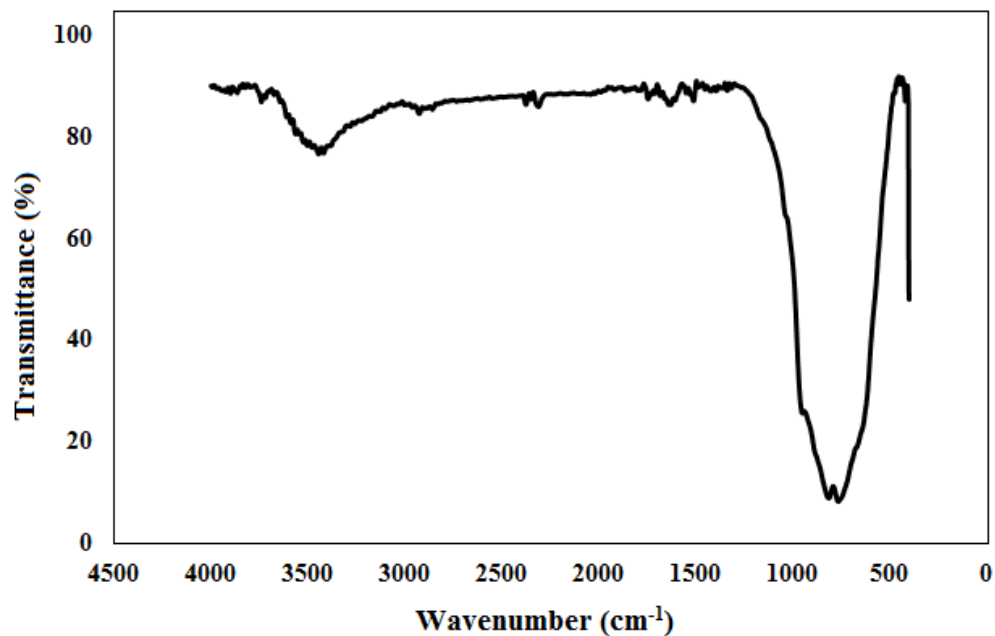


**Fig. 3.** FT-IR spectra the synthesized WO<sub>3</sub>.

DRS analysis was employed to characterize the light absorption properties of WO<sub>3</sub>. UV-vis DRS of the WO<sub>3</sub> catalyst in Fig. 4 showed an absorption maximum at 401 nm. According to literature, the oxygen ligand to metal charge transfer (LMCT) bands for W<sup>+6</sup>, appeared ~300-400 nm.

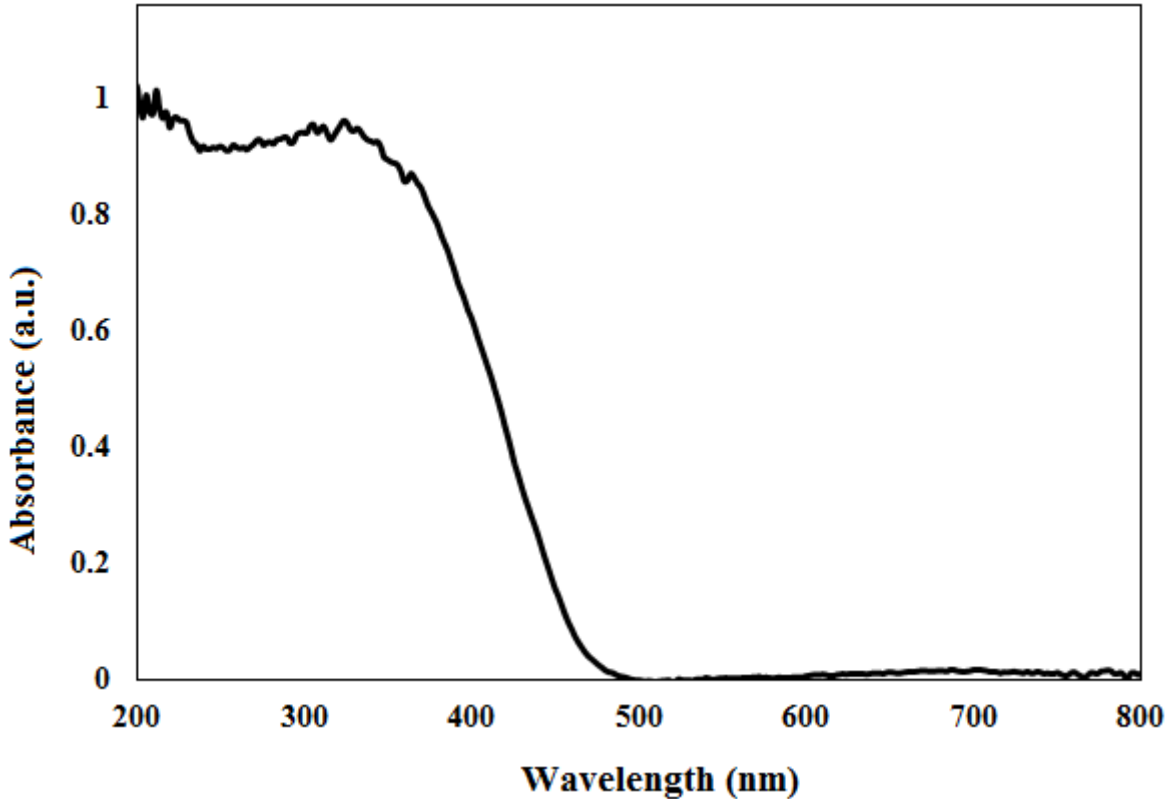


**Fig. 4.** UV-vis DRS spectrum WO<sub>3</sub> nanostructured catalyst.

Fig. 5 show that band gap of WO<sub>3</sub> was calculated 2.8 eV. Therefore, this photocatalyst can active in visible range.

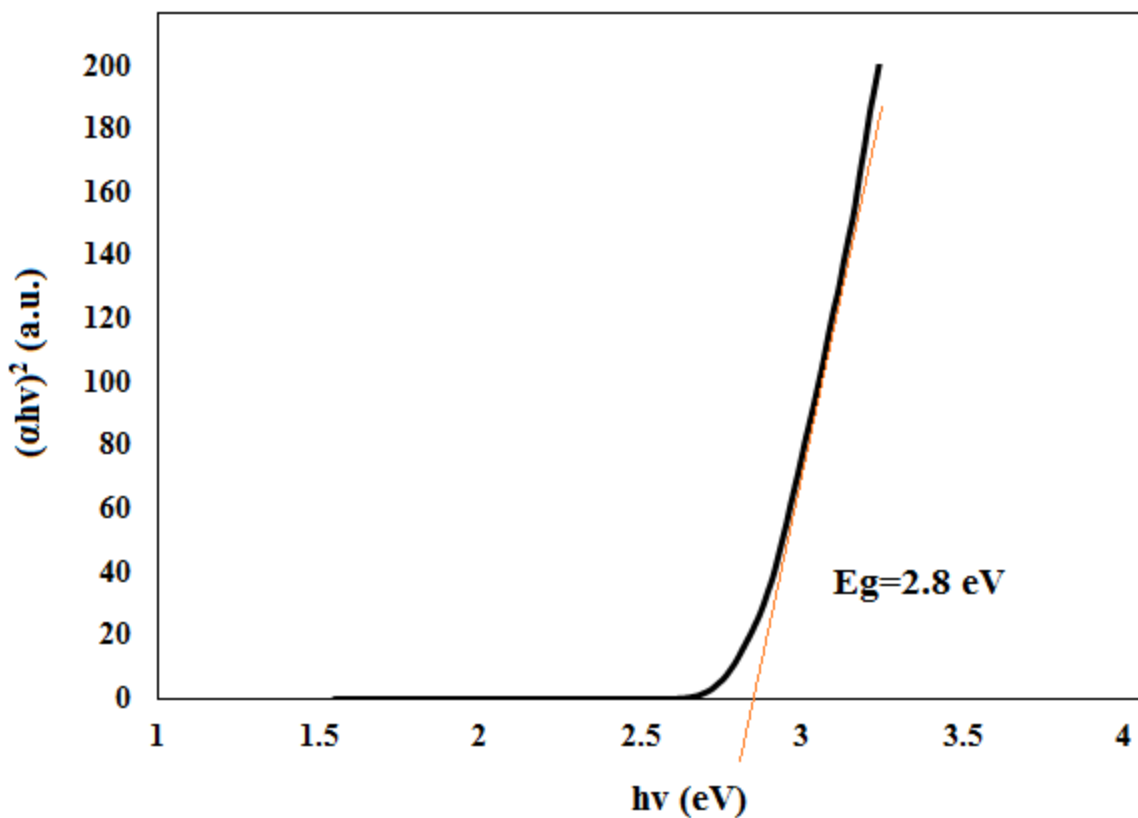


**Fig. 5.** The band gap of  $\text{WO}_3$ .

### **Photocatalytic degradation of methylene blue**

The photocatalytic activities of  $\text{WO}_3$  catalyst were evaluated by the degradation of MB in aqueous solution under LED visible light irradiation. The photocatalytic activity and adsorption property of  $\text{WO}_3$  was compared in Fig. 6. Removal of MB was carried out about 70% by adsorption on  $\text{WO}_3$ , but MB was degraded in the presence of  $\text{WO}_3$  under LED light irradiation about 90%.

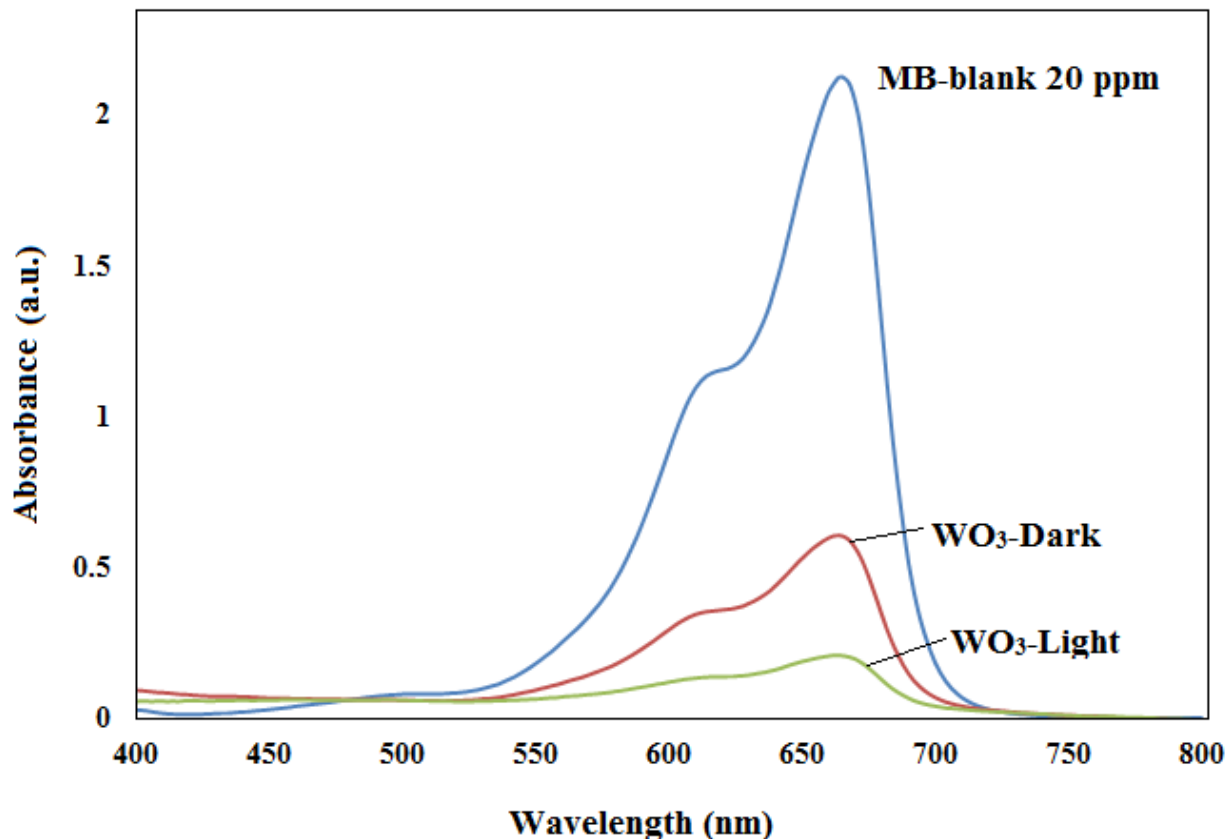
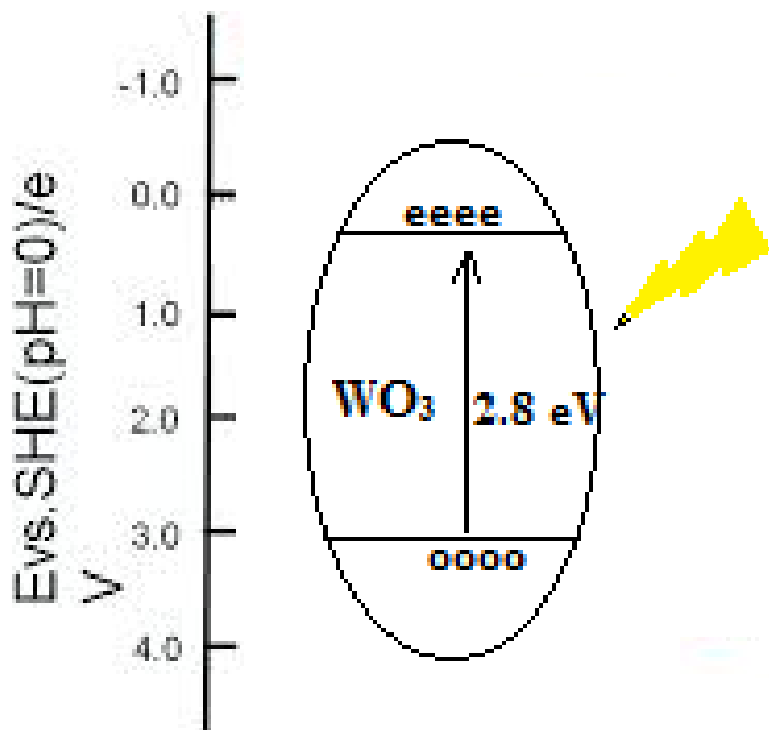


**Fig. 6.** UV-Vis spectra of MB (20 mg/L) in the presence of WO<sub>3</sub> at different conditions.

A possible mechanism has been shown in Scheme 1. It is well known that WO<sub>3</sub> has a low band gap of approximately 2.8 eV can effectively absorb visible range of sunlight. The electrons in the valence band (VB) of WO<sub>3</sub> are preferentially excited to its conduction band (CB) under visible light irradiation and therefore generate an equal amount of holes in its VB. The photoexcited electrons reduce molecular oxygen to the superoxide radicals. On the other hand, in aqueous medium, the holes in the valence band of WO<sub>3</sub> oxidize the water molecules to generate hydroxyl radicals. The hydroxyl radicals can convert to H<sub>2</sub>O<sub>2</sub> and superoxide radical anion to regenerate hydroxyl radicals. Finally, derived hydroxyl radicals decompose MB to carbon dioxides and water.





**Scheme 1.** The mechanism of MB photodegradation by  $\text{WO}_3$ .

## Conclusion

$\text{WO}_3$  as visible-light-driven photocatalysts was prepared by co-precipitation method. Visible light photocatalytic activity of the prepared catalyst was investigated by degradation of MB. After visible light irradiation for 1 h, about 90% of MB molecules were degraded on  $\text{WO}_3$ .

## References

- [1] Hoffmann, M. R.; Martin, S. T.; Choi, W.; Bahnemann, D. W. Environmental applications of semiconductor photocatalysis. *Chem. Rev.* **1995**, *95*, 69–96.
- [2] Kou, J.; Li, Z.; Yuan, Y.; Zhang, H.; Wang, Y.; Zou, Z. Visiblelight- induced photocatalytic oxidation of polycyclic aromatic hydrocarbons over tantalum oxynitride photocatalysts. *Environ. Sci. Technol.* **2009**, *43*, 2919–2924.

- [3] Park, Y.; Singh, N. J.; Kim, K. S.; Tachikawa, T.; Majima, T.; Choi, W. Fullerol-titania charge-transfer-mediated photocatalysis working under visible light. *Chem.sEur. J.* **2009**, *15*, 10843–10850.
- [4] Xin, G.; Guo, W.; Ma, T. Effect of annealing temperature on the photocatalytic activity of WO<sub>3</sub> for O<sub>2</sub> evolution. *Appl. Surf. Sci.* **2009**, *256*, 165–169.
- [5] Bamwenda, G. R.; Sayama, K.; Arakawa, H. The effect of selected reaction parameters on the photoproduction of oxygen and hydrogen from a WO<sub>3</sub>-Fe<sup>2+</sup>-Fe<sup>3+</sup> aqueous suspension. *J. Photochem. Photobiol., A* **1999**, *122*, 175–183.
- [6] Morales, W.; Cason, M.; Aina, O.; Tacconi, N. R. de; Rajeshwar, K. Combustion synthesis and characterization of nanocrystalline WO<sub>3</sub>. *J. Am. Chem. Soc.* **2008**, *130*, 6318–6319.
- [7] A. Kudo, Y. Miseki, *Chem. Soc. Rev.* 2009, *38*, 253.
- [8] F. Wang, C. Di Valentin, G. Pacchioni, *Phys. Rev. B* 2011, *84*, 073103.
- [9] Wang, F., Di Valentin, C. and Pacchioni, G., 2012. Rational band gap engineering of WO<sub>3</sub> photocatalyst for visible light water splitting. *ChemCatChem*, *4*(4), pp.476-478